GEOLOGICA CARPATHICA, APRIL 2005, 56, 2, 123–136

Jurassic radiolarian cherts in north-western Croatia: geochemistry, material provenance and depositional environment

JOSIP HALAMIĆ[1], VESNA MARCHIG[2] and ŠPELA GORIČAN[3]

[1]Institute of Geology, Sachsova 2, HR-10000 Zagreb, Croatia; jhalamic@igi.hr
[2]Bundesanstalt für Geowissenschaften und Rohstoffe, Stilleweg 2, D-30631 Hannover, Germany; v.marchig@bgr.de
[3]Institute of Paleontology, ZRC SAZU, Novi trg 2, SI-1000 Ljubljana, Slovenia; spela@zrc-sazu.si

(Manuscript received April 28, 2004; accepted in revised form June 16, 2004)

Abstract: The Middle Jurassic (uppermost Bajocian–lower Bathonian to upper Bathonian–lower Callovian) radiolarian cherts in the Medvednica Mt (NW Croatia) have a high content of SiO_2 (average 90.87 %). Most of the silica is of biogenic origin as is indicated by a high Si/Si+Al+Fe+Ca ratio (0.83–0.97). The Al/Al+Fe+Mn ratio (average 0.59) and relatively low contents of Fe and Mn suggest that the sedimentation of the radiolarian cherts was not influenced by hydrothermal volcanisms. The high correlation coefficient between the lithophile elements Ti, K, Al, Th, Zr, Hf and Rb implies that the detrital component in radiolarian cherts for the most part has a terrigenous provenance. The MnO/TiO_2 ratio and La_n/Ce_n vs. $Al_2O_3/(Al_2O_3+Fe_2O_3)$ diagram show that the investigated cherts were derived from two different, but not necessarily strongly separated, sedimentation areas: (1) continental shelf and slope or marginal sea, and (2) deep ocean floor, trench or basaltic plateau. According to the proposed sedimentation model the radiolarian cherts in the Medvednica Mt were deposited in a relatively narrow basin. The detrital material was derived from two source areas: (1) from a continent (terrigenous input) and (2) from an accretionary wedge (undifferentiated magmatic arc-like input). During the Late Jurassic–Early Cretaceous the radiolarian cherts were incorporated into the tectonic mélange (accretionary prism) along with other fragments: Triassic radiolarian cherts and carbonate rocks; Jurassic shales, siltites and sandstones and basic and ultrabasic magmatic rocks.

Key words: Jurassic, Croatia, south-western Pannonian region, major and trace elements, radiolarian chert geochemistry, REE.

Introduction

Cherts, radiolarian cherts and shale (radiolarite s.str.) accompanied by basic and ultrabasic magmatic rocks (pillow lavas, diabase, and serpentinite — Steinmanns trinity) often occur as smaller or bigger blocks in the ophiolitic mélange. These siliceous rocks are often deposited in association with magmatic rocks, and as a part of the ophiolite sequence (layer 1 — Wilson 1989) they play an important role in the paleogeographical reconstructions of the sedimentary environments. In many cases the radiolarian cherts are interlayered or incorporated between the basic volcanic rocks and their fossil content does not only determine their age, but the age of the effusive rocks, too.

More intensive geochemical research of continental siliceous sediments was induced during the research into pelagic sediments in the DSD Projects in the second half of the 20th century (Shimizu & Masuda 1977; Manetti et al. 1979; Barrett 1981; Rangin et al. 1981; Baltuck 1982; Sugisaki 1984; Adachi et al. 1986; Ruitz-Ortiz et al. 1989; Murray et al. 1990, 1991, 1992a,b,c; Murray 1994; Girty et al. 1996 and others). On the basis of comparison of geochemical data from pelagic sediments of recent oceans, this research tried to define the parameters for the determination of sedimentary environments and for the origin of older siliceous sediments on the continent. This type of research is very important for siliceous rocks we find in tectonic mélange today, that is in the former accretionary prisms. Detailed geochemical research of cherts, radiolarian cherts and shales (major, trace and rare earth elements) is still used today to geochemically determine their sedimentation environment, sedimentation conditions, and the provenance of the material they contain (Kunimaru et al. 1998; Dasgupta et al. 1999; Shimizu et al. 2001; Sugitani et al. 2002; Kato et al. 2002; Di Leo et al. 2002 and others).

Radiolarian cherts, that have been known in Medvednica Mt ever since the late 19th century (Pilar 1881), have been determined as older than Upper Cretaceous (Gorjanović-Kramberger 1908) or as Lower-Upper Cretaceous (Šikić et al. 1979; Basch 1983). The first geochemical and paleontological data for radiolarian cherts in the Medvednica Mt date back to the end of the last century (Halamić & Goričan 1995; Halamić et. al. 1995; Halamić 1998; Halamić et al. 1999). Through paleontological analyses it has been determined that the radiolarian cherts of the northwestern part of the Medvednica Mt, occurring in the tectonic mélange as blocks accompanied by basic magmatic rocks, belong to two stratigraphic levels. One of these is Middle to Upper Triassic, the other is Middle Jurassic. Geochemical characterization of the Triassic radiolarian cherts was given in Halamić et al. (2001). In the present paper we present the geochemical characteristics of the Jurassic radiolarian cherts. On the basis of geochemical analyses and other geological data, we attempt to determine the provenance of

the material and the sedimentary environment of the area of Medvednica Mt during the Jurassic. This paper deals only with the radiolarian cherts that are undoubtedly Jurassic according to paleontological analyses of radiolarians.

Geological outline and petrographic data

Geology. Medvednica Mt is situated in the SW part of the Pannonian region (Fig. 1a) as an isolated «island» of Paleozoic and Mesozoic rocks surrounded by Tertiary and Quaternary sediments (Fig. 1b). According to recent geotectonic interpretations, Medvednica Mt belongs to the Supradinaricum (Herak 1986), or to the Inner Dinarides Unit (sensu Herak et al. 1990). According to Hass et al. (1990, 1995, 2000) and Šikić (1995) Medvednica Mt is situated in the Mid-Transdanubian Zone (i.e. Zagorje-Mid Transdanubian Zone — Pamić & Tomljenović 1998), which is separated toward the north by the Periadriatic-Balaton Line from the Transdanubian Central Range Subunit, while toward the southeast it is detached from

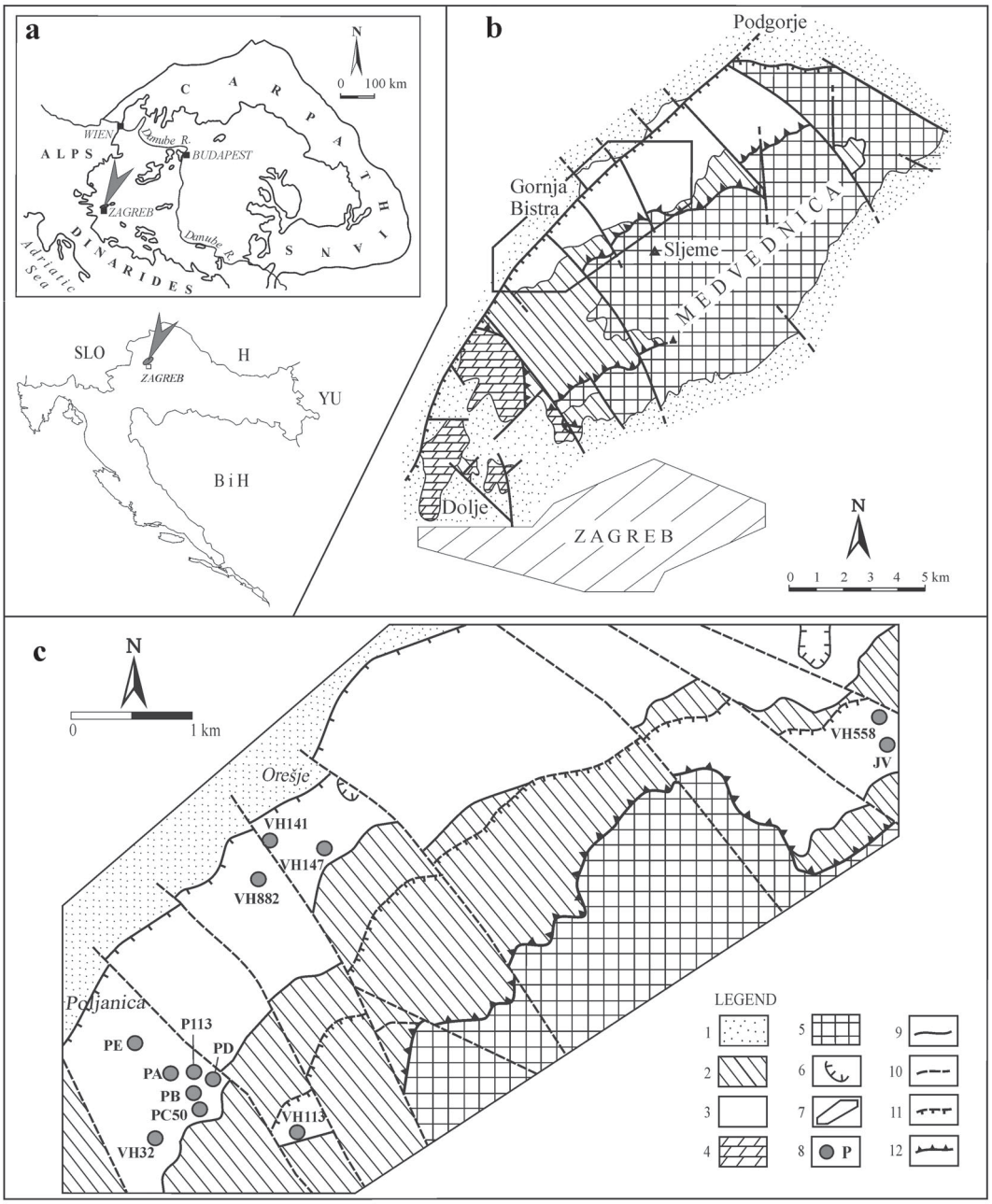

Fig. 1. a — Location map. **b** — Geological sketch map of Medvednica Mt. **c** — Simplified geological map of investigated area with sampling points (simplified after Šikić et al. 1977; Basch 1981, 1995; Halamić 1998). 1 — Neogene and Quaternary sediments, 2 — Cretaceous and Paleogene sedimentary rocks, 3 — Jurassic mélange, 4 — Triassic clastic and carbonate rocks of Zakičnica Nappe, 5 — low-grade metamorphic rocks, 6 — quarry, 7 — investigated area, 8 — sampling locations, 9 — stratigraphic boundary, 10 — fault, 11 — reverse fault, 12 — thrust fault.

the Tisza Megaunit by the Zagreb-Zemplen or Mid-Hungarian Line (Kovács et al. 1988).

The studied Jurassic radiolarian cherts are a part of the tectonic mélange, called the Repno Complex (Babić et al. 2002), which is built of a shale-siltite-sandy matrix with km-sized megablocks of pillow lavas, metabasalts and diabases, Triassic carbonates and Triassic and Jurassic radiolarian cherts, siltites and sandstones. This complex is situated in the northwestern part of the mountain where it occupies an area of around 25 km^2 (Fig. 1c) (Halamić 1998). The base of this unit is unknown because of its reverse contact with the surrounding rocks. On some localities, the mélange is overlain by deep-water calpionellid carbonates of the Tithonian-Berriasian age (exposed in the northern part of the Medvednica Mt and on the Ivanščica Mt), followed by the turbiditic rocks of the Lower Cretaceous age (Babić & Zupanič 1973; Halamić 1998). Towards the southeast, the tectonic mélange of the Medvednica Mt is partly in a reverse contact with the low-grade metamorphic complex, and partly unconformably overlain by Cretaceous–Paleogene sedimentary rocks. Towards the northeast it is separated by a normal fault from the metamorphic rocks (Fig. 1b). The radiolarites in the mélange in the Medvednica Mt are of the Triassic (Halamić & Goričan 1995) and Jurassic age (Halamić et al. 1999). The age of the shale was assumed to be the Upper Jurassic (Halamić 1998; Halamić et al. 1999) and it was later proven with palynomorphs to include Hettangian to Bajocian (Babić et al. 2002).

Jurassic radiolarian cherts in the northwestern part of Medvednica Mt are found in a two kilometers wide tectonized belt, between the Poljanica and the Bistra Valleys. Smaller occurrences of these rocks are also found in the right tributary stream of the Jelenja Voda Valley (Fig. 1c). These are exposed as decametric or hectometric blocks within a schistose sand-silt-shaly matrix accompanied by Triassic radiolarites and basic magmatic rocks. Matrix supported polymict conglomerates including Triassic limestone blocks are locally interstratified between the Jurassic cherts. This radiolarite-clastic succession was informally named the Poljanica unit (Halamić et al. 1999). The radiolarian analysis showed that the Jurassic samples belong to different zones (Table 1) and were deposited during the latest Bajocian–Early Bathonian (UA Zone 5) to the Late Bathonian–Early Callovian (UA Zone 7) (Halamić et al. 1999).

Petrography. The radiolarian cherts are very thin to thick-bedded (from 1 cm to a few decimeters) with wavy bedding surfaces (pinch and swell structure — according to Jenkyns & Winterer 1982) and alternate with millimeter- to centimeter-thick shale partings (Fig. 2). The rocks are dark or pale red, grey or pale grey, and greenish-grey (Table 2). The red colour depends on the quantity of the dispersed Fe-oxy-hydroxides (Fig. 3). Cherts are dissected by secondary microcrystal to granulated quartz veins. In the JV 1 and JV 2 samples veins of secondary calcite were registered. Mn-dendrites can be seen

Fig. 2. Rhythmically bedded sequence of radiolarite-siliceous silty shale, slightly tectonically deformed. Locality: Poljanica Valley, section PA (see Fig. 1c).

Table 1: Unitary association zones for analysed Jurassic radiolarian cherts of the Medvednica Mt (data from Halamić et al. 1999, UA Zones according to Baumgartner et al. 1995).

Sample	UA Zone	Age
PD0	5	latest Bajocian–early Bathonian
VH141	3–7	early-mid Bajocian to late Bathonian–early Callovian
VH882/1	5	latest Bajocian–early Bathonian
PA12	5	latest Bajocian–early Bathonian
VH113	5–7	latest Bajocian–early Bathonian to late Bathonian–early Callovian
PE1	6–7	mid Bathonian to late Bathonian–early Callovian
PC50	5	latest Bajocian–early Bathonian
PB6, PB18A	5	latest Bajocian–early Bathonian
P113/A9	5	latest Bajocian–early Bathonian
VH147A	5–7	latest Bajocian–early Bathonian to late Bathonian–early Callovian
VH32	5–8	latest Bajocian–early Bathonian to mid Callovian–early Oxfordian
VH558/5	7	late Bathonian–early Callovian
JVSP	5–7	latest Bajocian–early Bathonian to late Bathonian–early Callovian

Table 2: Microscopically determined lithology with rockcolour description.

Sample No.	Lithology	Colour
PD1	clayey radiolarian chert	dark red
PD2	radiolarite, laminated	grey
PD3	radiolarian chert	grey/red
PD4	clayey radiolarian chert	dark red
VH141	radiolarite	grey
VH141A	clayey radiolarian chert	pale red
VH882/1	radiolarian chert	dark red
VH882/2	radiolarite, laminated	grey/red
VH882/3	clayey radiolarian chert	dark red
PA5/1	chert with rare radiolarian tests	grey
PA7	radiolarian chert	pale grey
PA9	radiolarite	grey
PA15	clayey radiolarite	grey
PA20/1	radiolarian chert, sub-millimeter veins with manganese and megaquartz	gray/red
VH113	radiolarian claystone	dark grey
PE1/1	radiolarian chert	dark red
PE1/01	radiolarian chert, laminated	dark red
PC50	chert with rare radiolarian tests, brecciated	grey/red
PC50/1	radiolarian chert, brecciated	red
PB1	chert	dark red
PB3	chert with rare radiolarian tests	dark red
PB8	clayey radiolarian chert	dark red
PB19	radiolarite	greenish grey
P113/1	radiolarian claystone	light grey
P113/7	radiolarian chert, brecciated	grey
P113/9	radiolarian chert	red
P113/12A	radiolarian chert	grey
P113/13	clayey radiolarian chert	red
VH147	radiolarian chert	dark red
VH32/1	radiolarite	reddish grey
VH32/3	radiolarian chert	reddish grey
VH32/5	radiolarian chert	reddish grey
VH558A	clayey radiolarian chert	pale grey
VH558B	radiolarite, brecciated and veined by megaquartz	dark red
VH558C	radiolarian chert, laminated	dark red
VH558D	clayey chert with rare radiolarian tests	greenish grey
VH558/5	radiolarian chert	grey
JV1	radiolarian chert, dolomitized and veined by calcite	greeenish grey
JV2	radiolarian chert, veined by calcite	grey
JV3	chert with rare radiolarian tests	grey

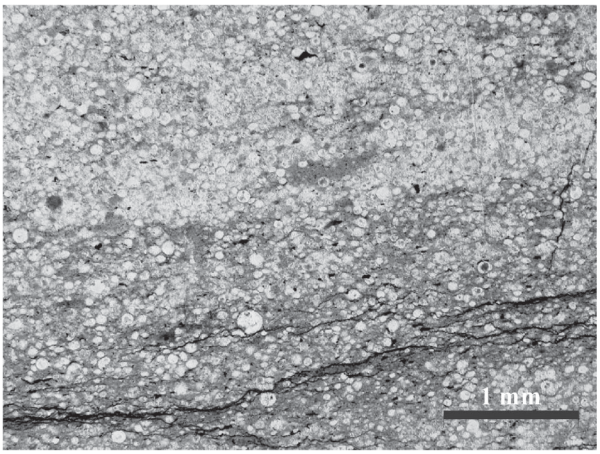

Fig. 3. Photomicrograph of a radiolarian chert. White circles are radiolarian tests. Grey coloured parts represent finely dispersed Fe-oxy-hydroxide in the siliceous matrix. Parallel polarizers (sample PA9).

on the bed surfaces, and manganese minerals can also be found in places in the sub-millimeter veins.

The cherts were microscopically determined as: (1) radiolarian cherts, (2) clayey radiolarian cherts and clayey cherts, (3) radiolarites s. str., (4) cherts with rare radiolarian tests and (5) cherts (Table 2). The matrix of the majority of samples is cryptocrystalline quartz, while the others have a microcrystalline texture. The radiolarian tests have different degrees of preservation and different size varying from 0.08 to 0.2 mm. The tests are filled with microcrystalline quartz and with relics of radial chalcedony. Some of these are partly filled with a greenish mineral (celadonite?) (samples VH882/3, PE1/1, PB3, P113/13). This greenish mineral can very rarely be found also as irregular masses in the chert matrix. Only a few radiolarian tests are impregnated with Fe-oxy-hydroxides. Other secondary minerals in the cherts are granules of detritic quartz resorbed on its edges, and also of white mica (sericite) with a maximum size of 0.05 mm. The accessory minerals are zircon (mostly rounded), hematite, and, very rarely, small apatite grains. In samples JV1 and JV2 the dolomitization and calcitization of cherts as tiny idiomorphic crystals of dolomite and calcite can be seen microscopically.

Materials and methods

In total, forty samples that were paleontologically determined as Jurassic were chosen for geochemical analysis. The

sampling locations are shown in Fig. 1c. For the microscopic analysis thin sections of all the samples were made.

Sample preparation. Only the rock pieces with the macroscopically smallest content of secondary quartz and calcite in submillimeter veins and of iron and manganese coatings on the cracks, were hand picked for chemical analysis. The chosen fragments were treated in diluted acetic acid for 12 hours to remove the majority of secondary calcite from the samples. After drying, the samples were powdered in an agate mortar.

Chemical analysis. The chemical analyses were performed in the BGR-Laboratory, Hannover, Germany by X-ray fluorescence (XRF) on Philips PW 1400 and PW 1480 instruments to determine the concentration of major and trace elements. The analytical method was calibrated with 106 international standards, and with 24 synthetic standards for elements or ranges of concentration not covered by international standards. Analytical precision was better than 2 % for major elements and better than 5 % for trace elements. Rare earth elements (REE), and also some trace elements with concentrations under the detection limit of the XRF method, were analysed by the inductivelly coupled plasma mass spectrometry (ICP-MS) method with the SCIEX 250 apparatus, following the pressure dissolution in hydrofluoric acid. The precision of this method was better than 5 %. The completeness of dissolution was checked by dissolving and analysing lithium tetraborate/metaborate rock-powder fused disks used by XRF.

Results and discussion

The major and trace elements of all analysed samples (40 in total) are listed in Table 3 and Table 4. The REE analytical data of the whole dataset are presented in Table 5. To maximize the comparisons with the published data cerium and europium anomalies were normalized against both NASC (North American shale composite — Gromet et al. 1984) and PAAS (post-Archean shales from Australia — Taylor & McLennan 1985). The anomalies were calculated as recommended by McLennan (1989) for europium and Murray et al. (1991) for cerium:

$$Eu/Eu^* = (Eu_{sample}/Eu_{shale})/(Sm_N \times Gd_N)^{0.5}$$
$$Ce/Ce^* = (Ce_{sample}/Ce_{shale})/(La_N \times Pr_N)^{0.5}$$

The samples in the sections were grouped to get a clearer statistical and graphical presentation of the analytical results. The results were grouped according to the geometric mean of the analysed values, and the calculated results are shown in Table 3 (for major elements), Table 4 (trace elements) and Table 5 (REE). The raw analytical data of major elements were recalculated on a volatile-free basis. Because of a closed data problem (compositional data) of major elements the log-ratio transformation ***log (x/y)*** (Aitchison 1986; Swan & Sandilands 1996) was carried out, with the SiO_2 as the denominator for all variables. The ratios of different elements and element groups are shown in Table 6.

Major elements

Silica. The SiO_2 content in all samples is relatively high and exceeds 90 % for most samples. The values vary from 81.4 % to 97.1 % (Table 3). The Si/Si+Al+Fe+Ca ratio was used to determine the provenance of the silica in the radiolarites. According to Ruitz-Ortiz et al. (1989) the typical biogenic silica-rich radiolarites have values of this ratio equal to 0.8–0.9. The acquired values range between 0.83 and 0.97 (Table 6), and correspond to cherts of which silica content is mainly of biogenic origin.

Aluminium, titanium and potassium are generally bonded to the aluminosilicate detritic phase, and as such they are good indicators of the terrigenous input into radiolarian cherts. Aluminium and titanium could be in part also located within clay minerals (Rangin et al. 1981). This group of major elements shows a very high mutual correlation coefficient (Table 7) that indicates their common provenance.

The aluminium content in some samples is relatively high. The values vary from 1.1 % to 8.5 %. This is the result of a higher content of detritic white mica (sericite), which can also be seen microscopically in thin sections. In addition to a relatively higher correlation coefficient to titanium and potassium, aluminium also shows a similar correlation coeffcient to iron and sodium ($r = 0.80$ and $r = 0.82$, respectively) (Table 7).

The titanium values in the samples range from 0.04 % to 0.28 %. In addition to its good correlation to aluminium and potassium, titanium also shows a high correlation coefficient to sodium ($r = 0.84$) (Table 7).

The K_2O contents in the analysed samples range between 0.174 % and 1.541 % (Table 3). Along with aluminium, sodium, titanium and rubidium, potassium is also a good indicator of the aluminosilicate component in the sediment (Murray et al. 1992c). Its terrigenous origin is indicated by the high correlation coefficients to aluminium, titanium and rubidium ($r = 0.93$, $r = 0.94$ and $r = 0.98$, respectively). Like aluminium and titanium, this element shows higher correlation to sodium ($r = 0.74$) (Table 7).

Iron and phosphorus. An increased content of iron in radiolarian cherts could indicate a stronger hydrothermal influence during the sedimentation, that is the relative distance of the sedimentation area from the mid-ocean ridge. Microscopic analyses of the thin sections have shown that most of the iron in the radiolarian cherts is in the form of a finely dispersed Fe-oxy-hydroxide (Fig. 3), and a lesser part in the form of hematite grains. The content of iron in the analysed samples varies from 0.5 % to 6.1 %. Iron, along with other major elements, has a distinctively negative correlation to silica, which is a consequence of an increased content of silica and the dilution of other elements (Table 7). Iron shows a relatively high positive correlation to magnesium ($r = 0.78$), which might be a consequence of an increased content of the greenish mineral (celadonite?) noticed in the thin sections and which probably originated from the altered volcanic fragments.

The phosphorus in the rock could be of dual origin. Firstly, it could be related to the products of an increased biogenic activity during sedimentation, and secondly, it could be a result of increased volcanic activity in the sedimentation basin. However, its flaw as an environmental indicator is that it migrates from the rock during the diagenetic processes, or is replaced by silica (dilution — according to Murray 1994). The phosphorus content in the analysed samples is relatively low and ranges from 0.007 % to 0.096 %. The reduced content of

Table 3: Major element data (wt. % — volatile free; Fe_2O_3* — Fe_{total}; Mean — Geometric mean). The mean values (bold numbers) were used for the construction of the discrimination diagrams.

Sample	SiO_2	TiO_2	Al_2O_3	Fe_2O_3*	MnO	MgO	CaO	Na_2O	K_2O	P_2O_5	LOI
PD1	86.39	0.27	6.81	3.55	0.074	0.85	0.182	0.26	1.541	0.054	2.683
PD2	91.49	0.18	5.05	1.07	0.049	0.56	0.132	0.25	1.190	0.032	2.084
PD3	89.80	0.22	5.50	2.03	0.074	0.75	0.138	0.22	1.208	0.040	2.352
PD4	94.56	0.13	3.28	0.92	0.026	0.19	0.090	0.07	0.756	0.030	1.557
Mean	**90.51**	**0.19**	**4.99**	**1.63**	**0.051**	**0.51**	**0.131**	**0.18**	**1.138**	**0.038**	**2.127**
VH141	93.09	0.10	3.31	1.88	0.051	0.67	0.143	0.11	0.604	0.032	1.826
VH141A	87.61	0.27	6.87	2.41	0.025	0.92	0.249	0.21	1.349	0.083	2.895
Mean	**90.31**	**0.16**	**4.77**	**2.13**	**0.036**	**0.79**	**0.189**	**0.15**	**0.903**	**0.052**	**2.299**
VH882/1	90.92	0.20	4.90	2.10	0.044	0.44	0.144	0.16	1.048	0.062	2.134
VH882/2	91.82	0.19	4.77	1.24	0.028	0.41	0.205	0.19	1.047	0.091	2.112
VH882/3	88.23	0.20	5.64	3.63	0.062	0.75	0.144	0.19	1.051	0.048	2.526
Mean	**90.31**	**0.20**	**5.09**	**2.11**	**0.042**	**0.51**	**0.162**	**0.18**	**1.049**	**0.065**	**2.250**
PA5/1	95.08	0.08	2.46	1.26	0.060	0.41	0.114	0.11	0.403	0.018	1.453
PA7	95.32	0.04	1.11	0.52	0.272	0.12	2.301	0.08	0.226	0.007	2.753
PA9	94.70	0.08	2.95	1.09	0.034	0.41	0.078	0.10	0.549	0.013	1.701
PA15	95.69	0.09	2.46	0.53	0.056	0.19	0.251	0.10	0.589	0.050	1.286
PA20/1	86.10	0.12	3.53	1.50	1.129	0.63	6.174	0.15	0.646	0.018	6.343
Mean	**93.30**	**0.08**	**2.34**	**0.89**	**0.129**	**0.30**	**0.501**	**0.11**	**0.453**	**0.017**	**2.233**
VH113	83.65	0.18	6.79	5.76	0.070	2.18	0.174	0.24	0.893	0.072	2.532
PE1/1	93.83	0.07	1.87	0.84	0.531	0.15	2.111	0.12	0.385	0.031	2.930
PE1/01	92.69	0.12	3.09	1.44	0.227	0.25	1.337	0.13	0.638	0.069	2.552
Mean	**93.26**	**0.09**	**2.40**	**1.10**	**0.347**	**0.19**	**1.680**	**0.12**	**0.496**	**0.046**	**2.734**
PC50	89.59	0.19	4.78	2.70	0.253	0.53	1.008	0.17	0.753	0.062	2.769
PC50/1	89.61	0.26	5.64	2.17	0.040	0.51	0.170	0.30	1.267	0.034	2.335
Mean	**89.60**	**0.22**	**5.19**	**2.42**	**0.101**	**0.52**	**0.414**	**0.23**	**0.977**	**0.046**	**2.543**
PB1	93.79	0.17	3.88	0.66	0.024	0.29	0.111	0.16	0.886	0.028	1.794
PB3	91.10	0.20	4.71	1.97	0.071	0.74	0.134	0.18	0.872	0.028	2.190
PB8	87.63	0.24	6.17	3.18	0.035	0.81	0.218	0.20	1.453	0.070	2.661
PB19	93.54	0.11	3.18	1.73	0.061	0.42	0.113	0.12	0.680	0.042	1.615
Mean	**91.48**	**0.17**	**4.35**	**1.64**	**0.044**	**0.52**	**0.138**	**0.16**	**0.935**	**0.039**	**2.027**
P113/1	81.38	0.28	8.50	6.08	0.234	1.16	0.546	0.28	1.498	0.036	3.423
P113/7	88.61	0.17	4.90	3.62	0.192	0.81	0.708	0.15	0.776	0.056	2.627
P113/9	92.63	0.12	3.26	2.68	0.070	0.32	0.109	0.12	0.671	0.017	1.636
P113/12A	94.27	0.13	3.23	0.93	0.052	0.31	0.179	0.16	0.655	0.086	1.548
P113/13	88.97	0.20	5.35	3.09	0.234	0.70	0.172	0.16	1.060	0.073	2.381
Mean	**89.06**	**0.17**	**4.72**	**2.79**	**0.131**	**0.58**	**0.265**	**0.17**	**0.885**	**0.046**	**2.222**
VH147	91.76	0.16	4.55	1.93	0.029	0.45	0.150	0.12	0.806	0.044	1.894
VH32/1	97.07	0.04	1.55	0.69	0.036	0.17	0.082	0.08	0.254	0.016	1.172
VH32/3	96.62	0.07	1.73	0.87	0.045	0.19	0.078	0.08	0.290	0.020	1.166
VH32/5	96.42	0.06	1.77	0.66	0.206	0.19	0.252	0.08	0.310	0.046	1.380
Mean	**96.70**	**0.06**	**1.68**	**0.73**	**0.069**	**0.18**	**0.117**	**0.08**	**0.284**	**0.025**	**1.235**
VH558A	91.89	0.16	4.43	2.09	0.123	0.14	0.149	0.16	0.786	0.062	1.873
VH558B	96.64	0.04	1.80	0.63	0.322	0.10	0.062	0.07	0.326	0.018	1.014
VH558C	89.43	0.20	5.34	2.71	0.375	0.46	0.123	0.10	1.240	0.028	1.803
VH558D	85.06	0.25	5.98	3.37	0.390	0.87	2.700	0.30	0.978	0.085	4.393
VH558/5	91.47	0.12	3.62	2.64	0.219	0.39	0.809	0.18	0.459	0.096	3.013
Mean	**90.82**	**0.13**	**3.92**	**2.00**	**0.263**	**0.29**	**0.301**	**0.14**	**0.677**	**0.048**	**2.144**
JV1	91.11	0.09	1.76	1.66	0.773	1.10	3.076	0.14	0.227	0.065	4.495
JV2	89.29	0.08	1.52	1.52	0.690	0.83	5.723	0.12	0.174	0.079	6.017
JV3	92.98	0.11	2.81	1.89	0.088	0.57	0.944	0.14	0.431	0.027	2.318
Mean	**91.11**	**0.09**	**1.96**	**1.68**	**0.361**	**0.80**	**2.552**	**0.13**	**0.257**	**0.052**	**3.973**

the phosphorus in the radiolarian cherts is visible from its negative correlation to silica ($r = -0.41$) (Table 7). The correlation coefficient of phosphorus and iron is not significant ($r = 0.33$) and it also shows no relevant correlation to other elements (Table 7).

Calcium, magnesium and manganese. The calcium content in the analysed samples varies from a low 0.06 % to a relatively high 6.17 %. The content of this element in most samples is relatively low and mainly below 0.5 % (Table 3). The increased content of calcium in a few samples is connected to its secondary appearance in the form of submillimeter veins (Table 2). Calcium has no positive correlation to any major elements aside from manganese ($r = 0.90$), even more so, in most cases it is negative (Table 7).

The average contents of magnesium are relatively low (Table 3). Increased values have been registered in only three samples, which also contain celadonite? minerals.

The manganese content in the analysed radiolarian cherts ranges from 0.025 % to 0.773 %. The correlation coefficient to most major elements is negative, except to calcium ($r = 0.90$) which could indicate that a part of the manganese is of secondary origin too, meaning that it migrated into the rock

Table 4: Trace element data (mg/kg; Mean — Geometric mean). The mean values (bold numbers) were used for the construction of the discrimination diagrams.

Sample	Ba	Co	Cr	Hf	Nb	Ni	Rb	Sc	Sr	Th	V	Y	Zr
PD1	130	19	39	1.14	3.4	37	2.1	7	37	3.70	59	15	51
PD2	102	12	29	0.87	2.9	16	34.2	4	29	2.67	48	8	36
PD3	114	15	31	1.16	3.2	30	37.3	5	27	3.19	49	13	43
PD4	93	**1**	26	0.61	1.7	11	21.6	4	32	1.87	28	9	24
Mean	**109**	**8**	**31**	**0.9**	**2.7**	**21**	**34.6**	**5**	**31**	**2.8**	**44**	**11**	**37**
VH141	98	15	21	1.49	1.3	24	17.5	3	24	1.83	36	6	17
VH141A	107	21	41	1.30	3.9	30	39.6	9	35	4.55	54	15	42
Mean	**102**	**18**	**29**	**1.4**	**2.3**	**27**	**26.3**	**5**	**29**	**2.9**	**44**	**9**	**27**
VH882/1	111	8	27	0.98	3.5	21	40.3	5	29	3.44	37	11	32
VH882/2	99	9	32	1.02	3.5	12	40.0	5	31	3.80	30	15	37
VH882/3	105	20	31	0.99	5.1	37	40.2	5	30	3.66	50	15	39
Mean	**105**	**11**	**30**	**1.0**	**4.0**	**21**	**40.2**	**5**	**30**	**3.6**	**38**	**14**	**36**
PA5/1	58	3	18	0.48	1.6	11	12.5	3	20	1.39	19	7	15
PA7	40	1	15	0.24	0.9	1	5.7	1	23	0.65	2	9	10
PA9	69	7	19	0.45	1.9	13	18.3	3	18	1.35	33	9	15
PA15	62	**1**	17	0.56	1.7	4	19.1	3	23	1.53	38	8	17
PA20/1	67	5	24	0.66	2.2	18	20.2	2	45	1.73	35	16	20
Mean	**58**	**3**	**18**	**0.5**	**1.6**	**6**	**13.8**	**2**	**24**	**1.3**	**18**	**9**	**15**
VH113	99	30	22	0.81	3.2	65	29.4	8	20	2.88	73	12	30
PE1/1	64	7	18	0.39	1.3	6	11.4	1	25	1.21	21	9	12
PE1/01	83	14	24	0.58	1.6	9	19.5	3	32	1.99	48	11	19
Mean	**73**	**10**	**21**	**0.5**	**1.4**	**7**	**14.9**	**2**	**28**	**1.6**	**32**	**10**	**15**
PC50	124	10	32	0.92	2.9	31	24.0	5	31	3.14	61	12	39
PC50/1	117	7	37	1.39	4.0	17	41.5	6	31	3.43	49	13	50
Mean	**120**	**8**	**34**	**1.1**	**3.4**	**23**	**31.6**	**5**	**31**	**3.3**	**55**	**12**	**44**
PB1	102	6	29	0.82	2.4	8	26.2	5	33	2.39	26	8	29
PB3	103	12	27	1.15	4.6	23	29.7	4	23	3.28	38	7	41
PB8	127	8	35	1.22	3.8	15	51.1	7	29	3.62	47	17	44
PB19	85	10	22	0.58	1.6	11	22.2	3	21	1.98	35	10	20
Mean	**103**	**9**	**28**	**0.9**	**2.9**	**13**	**30.7**	**5**	**26**	**2.7**	**36**	**10**	**32**
P113/1	205	32	39	1.42	5.1	53	45.9	8	31	4.84	91	15	56
P113/7	91	22	27	1.03	3.1	42	24.6	4	27	2.95	38	10	33
P113/9	77	1	18	0.65	2.1	15	21.2	3	19	1.70	29	5	22
P113/12A	78	11	23	0.73	2.0	10	19.8	6	24	2.22	34	11	27
P113/13	123	19	27	0.98	2.9	32	31.5	6	29	3.11	30	14	37
Mean	**107**	**11**	**26**	**0.9**	**2.8**	**25**	**27.2**	**5**	**26**	**2.8**	**40**	**10**	**33**
VH147	85	15	39	0.92	2.0	33	23.3	5	23	2.98	58	9	37
VH32/1	41	6	11	0.25	0.7	6	5.4	1	17	0.79	11	6	8
VH32/3	45	5	35	0.57	0.9	16	6.7	1	19	1.16	11	7	22
VH32/5	58	4	16	0.32	0.9	9	6.9	1	27	0.95	13	11	11
Mean	**47**	**5**	**18**	**0.4**	**0.8**	**10**	**6.3**	**1**	**21**	**1.0**	**12**	**8**	**12**
VH558A	96	5	24	0.77	2.5	16	22.5	4	31	2.59	36	11	32
VH558B	46	7	18	0.21	0.6	31	8.7	1	32	0.68	24	10	7
VH558C	124	23	33	1.09	2.8	64	49.1	6	87	3.14	32	12	38
VH558D	131	21	33	1.31	3.4	42	31.1	7	43	3.84	44	16	51
VH558/5	65	17	30	0.61	1.9	53	13.5	3	29	2.06	27	16	26
Mean	**86**	**12**	**27**	**0.7**	**1.9**	**37**	**20.9**	**3**	**40**	**2.1**	**32**	**13**	**26**
JV1	64	9	26	0.58	1.3	16	5.6	2	106	1.72	22	12	21
JV2	51	8	16	0.53	0.9	8	3.8	3	181	1.63	2	14	17
JV3	108	5	35	0.58	1.8	21	12.3	3	61	1.93	16	7	18
Mean	**71**	**7**	**24**	**0.6**	**1.3**	**14**	**6.4**	**3**	**105**	**1.8**	**9**	**11**	**19**

during the diagenetic or postdiagenetic processes (Mn-dendrites on the bed surfaces).

Trace elements

The contents of all trace elements in the analysed Jurassic radiolarian cherts are relatively low. During the diagenetic processes the enrichment of the radiolarian cherts with added SiO_2 from the shale partings causes the dilution of all other trace elements (Murray 1994). This is revealed by the highly negative correlation of silica to all trace elements (r = –0.20 to –0.79) (Table 7), and is clearly visible on the cluster diagram too (Fig. 4).

Trace and major elements on the cluster diagram can be divided into 5 groups reflecting their mutual connection (Fig. 4).

The biggest group showing a relatively high correlation consists of ***K, Rb, Ti, Zr, Th, Al, Nb, Hf, Na, V*** and ***Cr*** (Fig. 4). The lithophile elements Ti, K, Al, Th, Zr, Hf and Rb are most commonly transported into the sedimentation basin in a suspended form. Therefore, they serve as a good indicator of the terrigenous input, and indirectly they are an indicator of the distance of the sedimentation basin from the continent.

Table 5: Rare earth elements (mg/kg; Mean = Geometric mean). The mean values (bold numbers) were used for the construction of the discrimination diagrams.

Sample	La	Ce	Pr	Nd	Sm	Eu	Gd	Tb	Dy	Ho	Er	Tm	Yb	Lu	SumREE
PD1	12.30	27.5	2.99	11.6	2.41	0.53	2.10	0.31	1.84	0.36	1.08	0.15	1.01	0.18	64.36
PD2	9.03	20.8	2.39	8.46	1.50	0.29	1.15	0.15	1.04	0.20	0.69	0.10	0.70	0.13	46.63
PD3	7.90	16.5	2.15	7.98	1.57	0.39	1.58	0.24	1.43	0.29	0.85	0.13	0.81	0.16	41.98
PD4	5.14	10.3	1.53	5.53	1.04	0.23	1.08	0.16	0.89	0.20	0.58	0.091	0.53	0.11	27.51
Mean	**8.19**	**17.66**	**2.20**	**8.15**	**1.56**	**0.34**	**1.42**	**0.21**	**1.25**	**0.25**	**0.78**	**0.12**	**0.74**	**0.14**	**43.01**
VH141	3.78	7.6	1.02	4.13	0.85	0.20	0.88	0.13	0.82	0.15	0.44	0.067	0.46	0.096	20.58
VH141A	10.40	27.2	3.18	12.6	2.53	0.55	2.45	0.37	2.12	0.39	1.18	0.17	1.16	0.21	64.51
Mean	**6.27**	**14.34**	**1.80**	**7.21**	**1.47**	**0.33**	**1.47**	**0.22**	**1.32**	**0.24**	**0.72**	**0.11**	**0.73**	**0.14**	**36.37**
VH882/1	9.92	22.0	2.63	10.5	1.94	0.48	2.04	0.31	1.68	0.33	0.94	0.13	0.87	0.16	53.93
VH882/2	13.70	33.1	3.84	15.6	3.42	0.76	3.18	0.43	2.42	0.45	1.26	0.18	1.08	0.21	79.63
VH882/3	11.80	26.7	2.86	10.3	1.82	0.43	1.69	0.28	1.68	0.33	1.05	0.15	0.96	0.18	60.23
Mean	**11.70**	**26.89**	**3.07**	**11.90**	**2.29**	**0.54**	**2.22**	**0.33**	**1.90**	**0.37**	**1.08**	**0.15**	**0.97**	**0.18**	**63.59**
PA5/1	3.82	11.2	1.08	4.65	0.93	0.24	0.85	0.11	0.72	0.13	0.38	0.048	0.34	0.08	24.58
PA7	2.01	6.4	0.64	2.84	0.94	0.23	0.90	0.13	0.79	0.14	0.34	0.040	0.26	0.065	15.72
PA9	4.66	12.5	1.20	4.60	0.97	0.26	0.83	0.13	0.76	0.12	0.39	0.050	0.39	0.089	26.95
PA15	5.14	12.4	1.62	6.91	1.50	0.34	1.46	0.20	1.23	0.24	0.56	0.080	0.54	0.11	32.33
PA20/1	6.55	18.9	2.24	9.44	2.13	0.51	2.35	0.35	2.07	0.34	0.88	0.12	0.72	0.12	46.72
Mean	**4.13**	**11.60**	**1.25**	**5.24**	**1.22**	**0.30**	**1.17**	**0.17**	**1.02**	**0.18**	**0.48**	**0.06**	**0.42**	**0.09**	**27.33**
VH113	6.66	15.1	1.76	7.45	1.69	0.40	1.80	0.27	1.60	0.31	0.91	0.13	0.80	0.17	39.07
PE1/1	3.09	7.8	0.90	4.03	1.38	0.33	1.38	0.18	1.07	0.18	0.45	0.061	0.43	0.10	21.36
PE1/01	4.89	12.3	1.28	5.46	1.67	0.45	1.86	0.25	1.34	0.24	0.67	0.088	0.56	0.12	31.18
Mean	**3.89**	**9.78**	**1.07**	**4.69**	**1.52**	**0.39**	**1.60**	**0.21**	**1.20**	**0.21**	**0.55**	**0.07**	**0.49**	**0.11**	**25.78**
PC50	9.06	21.8	2.32	9.07	1.70	0.41	1.81	0.25	1.59	0.30	0.86	0.12	0.75	0.15	50.19
PC50/1	7.11	15.8	1.73	7.17	1.49	0.37	1.44	0.21	1.26	0.26	0.77	0.12	0.75	0.15	38.63
Mean	**8.03**	**18.56**	**2.00**	**8.06**	**1.59**	**0.39**	**1.61**	**0.23**	**1.42**	**0.28**	**0.81**	**0.12**	**0.75**	**0.15**	**44.00**
PB1	5.07	13.5	1.51	5.69	1.24	0.28	1.19	0.19	1.02	0.19	0.56	0.085	0.54	0.11	31.18
PB3	8.62	23.2	2.17	8.00	1.34	0.29	1.09	0.17	1.17	0.25	0.77	0.10	0.71	0.15	48.03
PB8	13.30	25.3	3.32	13.4	2.78	0.64	2.77	0.40	2.26	0.43	1.25	0.16	1.13	0.20	67.34
PB19	6.75	14.4	1.69	6.65	1.36	0.29	1.30	0.19	1.09	0.24	0.62	0.084	0.59	0.11	35.36
Mean	**7.91**	**18.38**	**2.07**	**7.98**	**1.58**	**0.35**	**1.47**	**0.22**	**1.31**	**0.26**	**0.76**	**0.10**	**0.71**	**0.14**	**43.24**
P113/1	14.80	40.1	3.60	13.7	2.36	0.46	2.02	0.29	1.83	0.39	1.23	0.19	1.20	0.23	82.40
P113/7	6.91	17.0	1.82	6.86	1.49	0.34	1.37	0.20	1.19	0.22	0.69	0.094	0.67	0.11	38.96
P113/9	4.46	10.8	1.01	3.40	0.71	0.13	0.59	0.092	0.58	0.12	0.44	0.053	0.40	0.089	22.87
P113/12A	7.29	17.7	2.33	9.95	2.22	0.48	2.12	0.30	1.69	0.31	0.88	0.11	0.66	0.13	46.17
P113/13	9.86	24.0	2.45	9.61	1.99	0.44	1.87	0.26	1.63	0.31	0.97	0.14	0.88	0.16	54.57
Mean	**8.00**	**19.91**	**2.07**	**7.89**	**1.62**	**0.34**	**1.45**	**0.21**	**1.28**	**0.25**	**0.80**	**0.11**	**0.71**	**0.14**	**44.78**
VH147	6.10	14.8	1.42	5.56	1.14	0.19	1.00	0.14	0.92	0.20	0.64	0.090	0.65	0.13	32.98
VH32/1	1.97	3.6	0.48	2.33	0.47	0.12	0.54	0.071	0.44	0.091	0.27	0.031	0.23	0.057	10.67
VH32/3	2.78	6.1	0.78	3.13	0.56	0.12	0.58	0.090	0.53	0.094	0.31	0.048	0.28	0.077	15.48
VH32/5	3.53	7.1	1.07	4.50	0.91	0.22	0.99	0.14	0.82	0.18	0.42	0.051	0.37	0.090	20.41
Mean	**2.66**	**5.37**	**0.74**	**3.20**	**0.62**	**0.15**	**0.68**	**0.10**	**0.58**	**0.12**	**0.33**	**0.04**	**0.29**	**0.07**	**14.97**
VH558A	6.60	15.5	1.87	7.77	1.65	0.38	1.64	0.23	1.43	0.26	0.88	0.11	0.70	0.14	39.16
VH558B	4.96	14.6	1.81	8.58	1.67	0.38	1.47	0.21	1.11	0.20	0.47	0.061	0.34	0.067	35.93
VH558C	14.30	41.3	4.34	16.0	2.54	0.51	1.92	0.28	1.56	0.32	1.01	0.13	1.05	0.16	85.42
VH558D	11.00	24.9	2.95	11.5	2.30	0.44	2.23	0.35	2.27	0.44	1.16	0.18	1.08	0.20	61.00
VH558/5	6.01	14.9	1.87	7.87	2.02	0.44	2.16	0.32	1.58	0.31	0.75	0.10	0.65	0.13	39.11
Mean	**7.91**	**20.32**	**2.41**	**9.93**	**2.01**	**0.43**	**1.86**	**0.27**	**1.55**	**0.30**	**0.82**	**0.11**	**0.71**	**0.13**	**48.76**
JV1	6.06	17.4	2.10	8.40	2.02	0.38	1.89	0.28	1.66	0.29	0.82	0.10	0.68	0.12	42.20
JV2	6.17	17.9	2.28	9.31	2.13	0.52	2.37	0.35	1.84	0.36	0.97	0.12	0.68	0.13	45.13
JV3	4.09	10.0	1.08	4.11	0.93	0.21	0.77	0.13	0.69	0.16	0.42	0.066	0.42	0.093	23.17
Mean	**5.35**	**14.60**	**1.73**	**6.85**	**1.59**	**0.35**	**1.51**	**0.23**	**1.28**	**0.26**	**0.69**	**0.09**	**0.58**	**0.11**	**35.22**

Chromium and vanadium containing minerals are relatively resistent to continental weathering, so they can also indirectly serve as indicators of the terrigenous input into the sediment even though they could also be enriched in hydrothermal precipitate (Gundlach & Marchig 1982). Al, K and Rb are mostly connected to the clayey fraction and show a high mutual correlation factor ($r_{Al-K}=0.93$; $r_{Al-Rb}=0.90$ and $r_{K-Rb}=0.98$). Ti, Zr, Hf, Th, V and Cr are contained in the heavy mineral fraction and their mutual correlation factor is also relatively high (Table 7).

The other group of trace elements showing a relatively high and significant mutual correlation consists of ***Co*** and ***Ni*** ($r=0.85$ — Table 7). These two elements also show a significant correlation to the major elements Fe and Mg (Fig. 4), where a part of the iron and nickel could also be derived from the hydrothermal component (Marchig et al. 1982). However, magnesium and cobalt should be interpreted with caution because of their migrability during diagenetic processes (Murray 1994).

The third group consists of the lithophile elements ***barium*** and ***scandium*** ($r=0.81$) and ***lanthanum*** ($r_{La-Ba}=0.79$ and $r_{La-Sc}=0.77$) (Fig. 4). In the magmatic rocks barium is accompanied by potassium, and these were geochemically separated in the hydrothermal phase. Despite its relatively high correla-

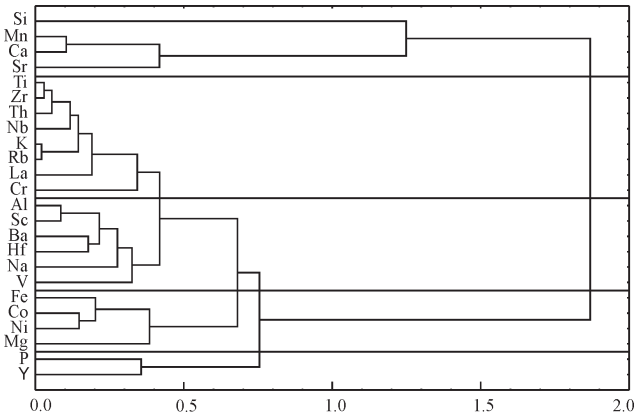

Fig. 4. Cluster analysis diagram of major and trace elements (Tree clustering; Linkage rule — Complete linkage; Distance measure — 1-Pearson r).

tion to potassium (r = 0.85), barium cannot be determined as uniquely of hydrothermal origin, because a part of it certainly derives from the detritic component (detrital clay minerals).

The next group consists of ***yttrium*** and the major element phosphorus (r = 0.64) (Table 7). These two elements in radiolarian cherts can be of dual origin. They can originate from hydrothermal solutions (adsorption from sea-water onto the ferric hydroxides precipitated from hydrothermal solutions) (Berner 1973) or they can be of biogenic origin. The yttrium and phosphorus in the investigated radiolarian cherts are most probably of hydrothermal origin, because the average content of yttrium is low (average = 11 mg/kg), which is very close to the values for the hydrothermal metalliferous sediments from the Red Sea. The siliceous rocks with apatite of biogenic origin have much higher contents of yttrium (Marchig et al. 1982).

The trace element ***strontium*** is most probably connected to the carbonate component in the radiolarian cherts, and is indirectly a part of the fifth group of major elements in the cluster diagram (Fig. 4) along with calcium and manganese. Because these two elements most probably have a secondary origin (calcite veins, manganese coatings and microscopically visible calcitization), strontium is also most probably bonded to the secondary calcite.

REE

When compared to the content of REE in post-Archean average Australian shale (183 mg/kg) (Taylor & McLennan 1985), North American shale composite (173 mg/kg) (Gromet et al. 1984) and European shale (204 mg/kg) (Haskin & Haskin 1966), the total content of REE in the studied Jurassic radiolarian cherts is considerably lower and ranges from 10.7 to 85.4 mg/kg (Table 5). Most REE are transported into the sedimentation basin in a terrigenous fraction, i.e. it is for the most part connected to the silty-clayey component (McLennan 1989). The terrigenous provenance of REE in the investigated radiolarian cherts is also indicated by a significant positive correlation of ΣREE to terrigenous major elements K, Ti and Al (r = 0.76, r = 0.77 and r = 0.76, respectively). The trace elements connected to the detritic component also show a high correlation coefficient to the total content of REE (La — r = 0.98; Hf — r = 0.65; Rb — r = 0.80; Th — r = 0.83; Y — r = 0.74 and Zr — r = 0.76) (Table 7).

The distribution pattern on Fig. 5a diagram shows LREE enrichment compared to HREE (Chondrite normalization). Ce anomaly is positive except for three groups of samples (PD, VH141, VH32) (Table 6). On Fig. 5b the distribution patterns show positive Ce and Eu anomalies.

Material provenance and depositional environments

Material provenance. The studied Jurassic radiolarian cherts in the Medvednica Mt are placed in a tectonic mélange as smaller or larger blocks, so it is not possible to study their primary relations to the overlying or underlying sediments. However, they do carry paleontological and geochemical information that make good stratigraphic and environmental indicators for the paleogeographic reconstruction of the depositional area.

The cherts of the Medvednica Mt are rich in silica (average 90.87 %). The Si/Si+Al+Fe+Ca ratios (Table 6) (silica in rela-

Table 6: Ratio values used in the paper ([1] — NASC normalized; [2] — PAAS normalized). $Ce/Ce^* = (Ce_{sample}/Ce_{shale})/(La_N \times Pr_N)^{1/2}$. $Eu/Eu^* = (Eu_{sample}/Eu_{shale})/(Sm_N \times Gd_N)^{1/2}$.

	PD	VH141	VH882	PA	VH113	PE	PC	PB	P113	VH147	VH32	VH558	JV
Si/Si+Al+Fe+Ca	0.92	0.91	0.91	0.95	0.83	0.93	0.90	0.92	0.90	0.92	0.97	0.92	0.91
Al/Al+Fe+Mn	0.69	0.62	0.64	0.63	0.47	0.55	0.61	0.66	0.55	0.64	0.61	0.56	0.42
Al_2O_3/TiO_2	26.26	29.81	25.45	29.25	37.72	26.67	23.59	25.59	27.76	28.44	28.00	30.15	21.78
MnO/TiO_2	0.27	0.23	0.21	1.61	0.39	3.86	0.46	0.26	0.77	0.18	1.15	2.02	4.01
Zr/TiO_2	0.019	0.017	0.018	0.019	0.017	0.017	0.020	0.019	0.019	0.023	0.020	0.020	0.021
Th/Sc	0.55	0.58	0.73	0.63	0.36	0.78	0.66	0.55	0.56	0.60	0.95	0.71	0.59
La_n/Ce_n [1)]	1.06	1.00	0.99	0.81	1.01	0.91	0.99	0.98	0.92	0.94	1.14	0.89	0.84
Ce/Ce* [1)]	0.91	0.93	0.98	1.11	0.96	1.04	1.01	0.99	1.06	1.09	0.83	1.01	1.04
Ce/Ce* [2)]	0.96	0.98	1.03	1.17	1.01	1.10	1.07	1.05	1.13	1.16	0.88	1.06	1.09
Eu/Eu* [1)]	1.01	0.99	1.05	1.11	1.00	1.08	1.06	1.01	0.96	0.78	0.99	0.97	0.98
Eu/Eu* [2)]	1.07	1.05	1.12	1.18	1.07	1.15	1.13	1.07	1.03	0.83	1.05	1.03	1.04
$(La/Yb)_n$ [1)]	1.07	0.83	1.18	0.95	0.81	0.77	1.04	1.08	1.08	0.91	0.90	1.09	0.89
$(La/Yb)_n$ [2)]	0.82	0.63	0.90	0.72	0.62	0.58	0.79	0.82	0.83	0.69	0.69	0.83	0.69
$Al_2O_3/(Al_2O_3+Fe_2O_3)$	0.75	0.69	0.71	0.72	0.54	0.69	0.68	0.73	0.63	0.70	0.70	0.66	0.54
$V+Ni+Cr/Al_2O_3$	19.24	20.96	17.49	17.95	23.56	25.00	21.58	17.70	19.28	28.57	23.81	24.49	23.98

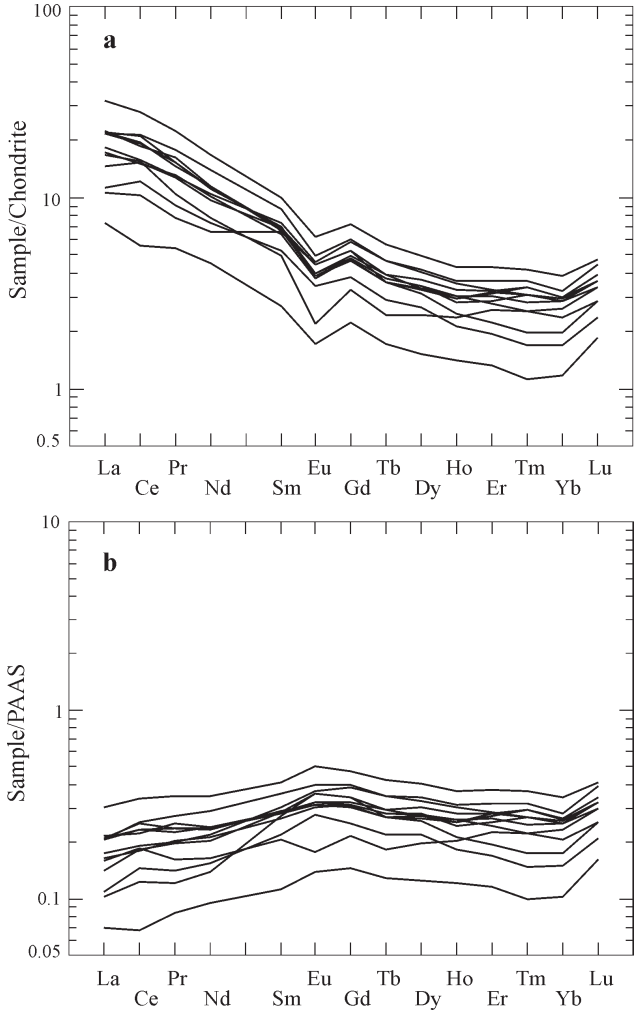

Fig. 5. Chondrite and PAAS normalized REE distribution diagrams for thirteen groups of analysed radiolarian cherts (PAAS values from McLennan 1989).

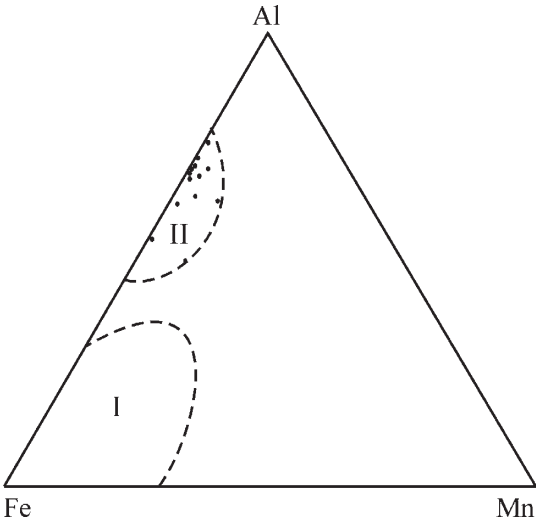

Fig. 6. Fe-Al-Mn diagram (Adachi et al. 1986). I — Hydrothermal field; II — Non-hydrothermal field.

Table 7: Correlation coefficient (r) for the major and trace elements, and ΣREE (N = 40; Significant correlation at p< 0.05; - — indicates negative correlation).

	SiO_2	TiO_2	Al_2O_3	Fe_2O_3	MnO	MgO	CaO	Na_2O	K_2O	P_2O_5	Ba	Co	Cr	Hf	La	Nb	Ni	Rb	Sc	Sr	Th	V	Y	Zr	ΣREE
SiO_2	1																								
TiO_2	–0.78	1																							
Al_2O_3	–0.83	0.95	1																						
Fe_2O_3	–0.87	0.68	0.80	1																					
MnO	–0.24	–0.22	–0.25	–0.04	1																				
MgO	–0.80	0.50	0.61	0.78	0.11	1																			
CaO	–0.25	–0.22	–0.28	–0.09	0.90	0.14	1																		
Na_2O	–0.78	0.84	0.82	0.64	–0.09	0.59	–0.03	1																	
K_2O	–0.68	0.94	0.93	0.59	–0.32	0.40	–0.35	0.74	1																
P_2O_5	–0.41	0.40	0.36	0.33	0.02	0.36	0.09	0.42	0.25	1															
Ba	–0.74	0.88	0.89	0.72	–0.20	0.47	–0.24	0.72	0.85	0.25	1														
Co	–0.76	0.62	0.75	0.82	–0.03	0.71	–0.12	0.58	0.56	0.41	0.63	1													
Cr	–0.56	0.79	0.73	0.48	–0.19	0.32	–0.20	0.63	0.72	0.29	0.70	0.49	1												
Hf	–0.69	0.88	0.84	0.61	–0.22	0.49	–0.20	0.73	0.82	0.32	0.82	0.61	0.72	1											
La	–0.72	0.84	0.82	0.61	–0.04	0.43	–0.11	0.64	0.84	0.45	0.79	0.61	0.66	0.72	1										
Nb	–0.75	0.91	0.90	0.69	–0.24	0.51	–0.23	0.78	0.86	0.29	0.81	0.59	0.66	0.80	0.81	1									
Ni	–0.68	0.53	0.67	0.80	0.02	0.62	–0.15	0.45	0.46	0.27	0.54	0.85	0.49	0.49	0.54	0.50	1								
Rb	–0.66	0.92	0.90	0.59	–0.30	0.38	–0.34	0.69	0.98	0.25	0.82	0.54	0.69	0.80	0.88	0.86	0.47	1							
Sc	–0.76	0.90	0.91	0.70	–0.29	0.61	–0.25	0.75	0.86	0.50	0.81	0.68	0.68	0.79	0.77	0.79	0.56	0.83	1						
Sr	–0.20	–0.07	–0.17	–0.01	0.58	0.21	0.65	–0.05	–0.19	0.23	–0.07	0.02	–0.02	–0.05	0.12	–0.16	0.02	–0.15	–0.04	1					
Th	–0.79	0.97	0.94	0.70	–0.22	0.53	–0.21	0.80	0.89	0.48	0.87	0.68	0.79	0.87	0.88	0.92	0.55	0.88	0.90	–0.03	1				
V	–0.72	0.76	0.86	0.73	–0.22	0.58-	–0.27	0.70	0.76	0.26	0.77	0.69	0.58	0.67	0.61	0.73	0.58	0.71	0.75	–0.29	0.76	1			
Y	–0.70	0.58	0.56	0.49	0.34	0.42	0.32	0.58	0.50	0.64	0.44	0.48	0.47	0.42	0.69	0.51	0.42	0.52	0.55	0.26	0.59	0.40	1		
Zr	–0.76	0.97	0.91	0.66	–0.21	0.47	–0.20	0.84	0.89	0.39	0.86	0.61	0.82	0.87	0.83	0.88	0.54	0.86	0.85	–0.05	0.94	0.73	0.57	1	
ΣREE	–0.72	0.77	0.76	0.56	0.10	0.43	0.01	0.60	0.76	0.49	0.72	0.61	0.61	0.65	0.98	0.74	0.54	0.80	0.74	0.23	0.83	0.55	0.74	0.76	1

tion to aluminosilicates and ferruginous and calcite minerals), show that most of the SiO_2 in the rock is of biogenic origin. Namely, the values of this ratio for biogenic silica rich cherts range from 0.8 to 0.9 (Ruitz-Ortiz et al. 1989). Higher values from the studied cherts in the Medvednica Mt (average 0.92) can be interpreted as a result of the enrichment of the chert beds with additional SiO_2 from the shale partings during diagenetic processes (Murray 1994). The enrichment of the radiolarite with additional silica and the dilution of other major and trace elements is also indicated by the high mutual negative correlation coefficient (see Table 7).

In their study of Triassic and Cretaceous cherts in central Japan, and of Cretaceous cherts and porcellanite from Pacific drill cores (Deep Sea Drilling Project) Sugisaki et al. (1982) and Adachi et al. (1986) showed that manganese is a relatively good indicator for determination of the hydrothermal component in the rock, while titanium is characteristic of the terrigenous input. Murray (1994) argued and stated that the manganese migrates during diagenesis. However, according to the newer studies of Permian and Triassic cherts conducted in southwest Japan by Kunimaru et al. (1998) and Shimizu et al. (2001), manganese in fact can be used as an indicator of a material provenance. Using a Mn-Al-Fe diagram proposed by Adachi et al. (1986) all the analysed samples fall in the non-hydrothermal field (Fig. 6), which indicates that the cherts were deposited in an area relatively distant from the hydrothermal influence. The Al/Al+Fe+Mn ratio could also be a measure of the hydrothermal or continental contribution to the sediment, the lower values indicating a hydrothermal input (Baltuck 1982; Adachi et al. 1986). The average value of this ratio for the radiolarian cherts of the Medvednica Mt is 0.59, which is very close to the value for the deep-sea clay (0.54) (Bostrom 1976), and slightly lower than the value of 0.619 (average for the shale composite) typical of the continental material (Baltuck 1982). It is interesting that the Middle to Upper Jurassic cherts of southern Spain have quite similar Al/Al+Fe+Mn ratio values (average 0.60 — Ruitz-Ortiz et al. 1989) to the values of the Medvednica Mt. Further on, the Fe and Mn contents in radiolarian cherts of the Medvednica Mt are relatively low, which indicates that they were probably deposited further from the influence of the hydrothermal volcanism, and probably closer to the continent (see Table 3). For the discrimination of the input of terrigenous material in relation to the volcaniclastic material, we used Zr/TiO_2 vs. $(V+Ni+Cr)/Al_2O_3$ diagram (Fig. 7) (Andreozzi et al. 1997). The ratio of these groups of elements shows that all analysed samples fall exclusively within the field of rocks deposited under the strong influence of the terrigenous input.

According to the noted values by McLennan et al. (1993) and Girty et al. (1996) the acquired values for the Al_2O_3/TiO_2 ratio (average 27.70), Th/Sc ratio (average 0.60) and Eu anomalies (PAAS normalized — average 1.06; NASC normalized — average 0.99) show that there has been mixing of materials from two sources. A part of it probably comes from an area built of differentiated upper continental crust, and the other part from an area characteristic of undifferentiated magmatic arc built mainly of basic to neutral magmatic rocks.

Depositional environment. The Ce anomaly values of analysed samples range from 0.83 to 1.11 (average 0.99) (Table 6)

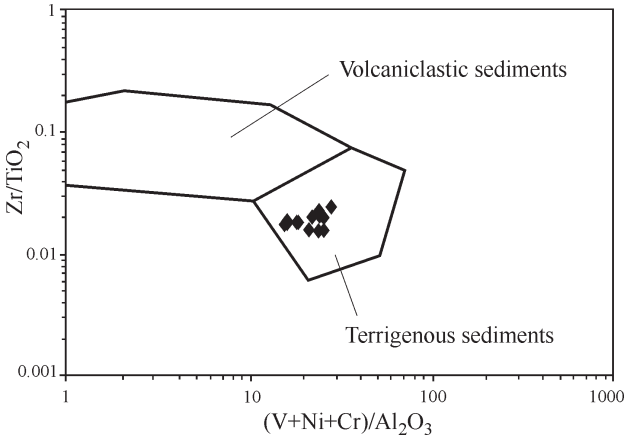

Fig. 7. Zr/TiO_2 *vs.* $(V+Ni+Cr)/Al_2O_3$ discrimination diagram (after Andreozzi et al. 1997). All samples are in the field of terrigenous origin of material in radiolarian cherts.

and indicate a sedimentation of the cherts in a continental margin area. As noted by Murray et al. (1990, 1992c) the near spreading ridge sediments, ocean-basin floor sediments, and continental margin sediments have Ce anomalies ~0.29, ~0.55 and 0.90 to 1.30, respectively. According to Dasgupta et al. (1999), a CaO/(CaO+MgO) ratio of >0.70 is characteristic of the fresh water environment while <0.50 is characteristic of the saline water environment. The ratios CaO/(CaO+MgO) (Table 6) for the majority of the studied Jurassic cherts suggest sedimentation in saline water. The increased values of this ratio in samples PE and JV (Table 6) are the consequence of the secondary calcite.

On the basis of the MnO/TiO_2 ratio, the studied rocks of the Medvednica Mt can be classified in two groups. The values of one group range from 0.18 to 0.46 while the other group ranges from 0.77 to 4.01 (Table 6). Sugisaki et al. (1982), Kunimaru et al. (1998) and Shimizu et al. (2001) stated that the values of the MnO/TiO_2 ratio lower than 0.5 are characteristic of areas of the continental shelf, continental slope, marginal seas, or of areas around basaltic islands, while the values of >0.5 are typical of deep ocean floor, trench or basaltic plateau sediments. The differentiation of the analysed cherts concerning their depositional environment is also visible on the discrimination diagram La_n/Ce_n vs. $Al_2O_3/(Al_2O_3+Fe_2O_3)$ (NASC normalized) proposed by Murray (1994), and supplemented by Girty et al. (1996) (Fig. 8). This diagram shows that most of the Jurassic radiolarian cherts fall into the field characteristic of sediments of the continental margin, while a part of it covers the field of island arc provenance with a tendency to the ocean island field.

On the basis of presented discrimination diagrams, the considered ratios of certain elements or groups of elements that we used as depositional environment indicators, detailed geological field studies and geochemical works for the Medvednica area (Halamić 1998), as well as on the basis of newer studies that dealt with the geodynamic evolution of this area during the Jurassic (Halamić et al. 1999; Pamić et al. 2002; Babić et al. 2002), we constructed a hypothetical model of the depositional area in the time of sedimentation of the studied Middle Jurassic radiolarian cherts (Fig. 9).

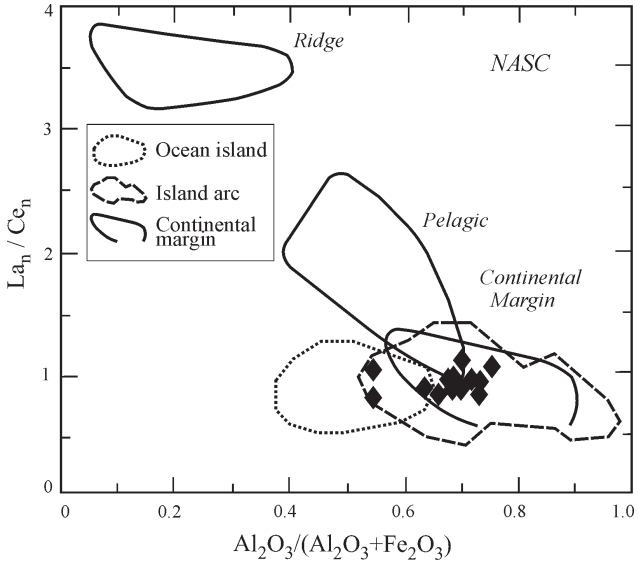

Fig. 8. La_n/Ce_n vs. $Al_2O_3/(Al_2O_3+Fe_2O_3)$ diagram (Murray 1994; Girty et al. 1996). The radiolarian cherts of Medvednica Mt are for the most part grouped in the continental margin field, but with a tendency to the island arc or ocean island field (NASC normalized).

Paleogeographic distribution of continents and oceans during the late Early and Middle Jurassic was determined by the onset of sea-floor spreading in the Central Atlantic, the Alpine Tethys and the Vardar Ocean, and synchronously, by subduction processes in the pre-existing oceanic basins (Stampfli & Borel 2004). Subduction processes in the investigated area were initiated probably already during the early Middle Jurassic. Wrenched-off pieces of the subducted oceanic crust along with their sedimentary cover and obducted parts of the continental crust were built into the subduction complex (accretionary prism) (Fig. 9). By further uplifting of the accretionary wedge weathering of obducted magmatic rocks and overlying sediments (oceanic crust) was enhanced. This weathered material was transported into the basin as an undifferentiated magmatic arc-like input (Fig. 9). The complex structure of the accretionary wedge, formed of magmatic and sedimentary rocks, explains the differentiation of the analysed MnO/TiO_2 and the La_n/Ce_n vs. $Al_2O_3/(Al_2O_3+Fe_2O_3)$ ratios of cherts in two different groups (see above). At the same time, due to compression and uplifting, on the opposite side of the subduction complex, on the continent, detritic terrigenous material was eroded and transported into the basin where radiolarian cherts accumulated (continental material supply) (Fig. 9).

The closing of the ocean area in these terrains continued during the Late Jurassic, and during these processes Triassic and Jurassic radiolarian cherts, Triassic magmatic and carbonate rocks and Jurassic clastic sediments (shales, siltites and sandstones) were all incorporated into the accretionary prism. The closing of the main basin, caused by the progress of the subduction processes, ended during the late Late Jurassic with the formation of a tectonic mélange (Halamić 1998; Babić et al. 2002) consisting of carbonate, siliceous and magmatic rocks of the Triassic age and clastic and siliceous rocks of the Jurassic age. At the same time, a peripheral compression foreland basin has been formed (Halamić 1998; Babić et al. 2002) (i.e. piggyback basin — Ori & Friend 1984; Allen & Allen 1990). In this basin the shallow-water turbidites of Early Cretaceous age were sedimented. The analysis of the mineral composition of the sandstones from these turbidites showed that the parent material was composed of sandstones, shales, cherts, basic and ultrabasic magmatic rocks, and to a lesser extent of low-grade metamorphic rocks. Most of the heavy mineral fraction in these rocks consists of chromspinell originating from ophiolithic rocks (Crnjaković 1987, 1989). Such a group of source rocks matches the composition of the rocks incorporated into the accretionary prism during the Middle and Late Jurassic.

The final closure, that is the collision and formation of a typical subduction-accretionary complex in the Medvednica Mt area took place in the lower part of the early Late Cretaceous (Halamić 1998; Babić et al. 2002).

Conclusions

The Jurassic radiolarian cherts of the Medvednica Mt have a high content of SiO_2 (average 90.87 %), and most of the silica is of biogenic origin. Such a provenance is indicated by a high Si/Si+Al+Fe+Ca ratio. The higher contents of SiO_2 in chert-beds diluted the contents of the other elements (negative correlation coefficient of all major, trace and rare earth elements with SiO_2) (Table 7).

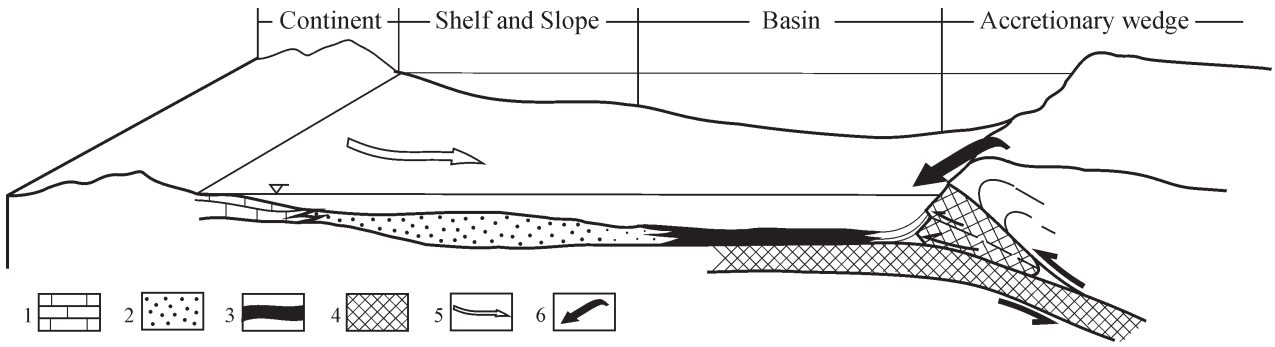

Fig. 9. Hypothetical model of sedimentation basin in the Middle–Upper Jurassic for the Medvednica Mt area. **1** — carbonate rocks, **2** — clastic rocks (shale, siltstone and sandstone), **3** — radiolarian ooze, **4** — oceanic crust, **5** — continental material supply, **6** — material supply from the accretionary wedge (Continental material-like supply mixed with the material of the obducted parts of the oceanic crust).

According to the Al/Al+Fe+Mn ratio and Mn-Al-Fe diagram the depositional area of the radiolarian cherts was relatively distant from the hydrothermal influence. The high positive correlation coefficient between the lithophile elements Ti, K, Al, Th, Zr, Hf and Rb and the Zr/TiO_2 vs. $(V+Ni+Cr)/Al_2O_3$ diagram show that the detrital material in the radiolarian cherts has a terrigenous origin.

The Al_2O_3/TiO_2 ratios and the Eu anomalies indicate provenance of the detritus in the radiolarian cherts from an undifferentiated magmatic arc, but the Th/Sc ratios suggest a source from a differentiated upper continental crust.

The Ce anomalies indicate sedimentation in the continental margin area, but the MnO/TiO_2 ratio shows that the Jurassic radiolarian cherts were derived from two different sedimentation areas: (1) continental shelf and slope, or marginal sea and (2) deep ocean floor, trench or basaltic plateau. The two different depositional areas (continental margin and island arc and the ocean island, respectively) are also indicated by the La_n/Ce_n vs. $Al_2O_3/(Al_2O_3+Fe_2O_3)$ ratio.

On the basis of geochemical data, field work and published data, a hypothetical model of the depositional basin during the deposition of the radiolarian cherts, was constructed. We suppose that the analysed rocks deposited in a relatively narrow sedimentary basin and that their detritic material derived from two different source areas: (1) from a continent (terrigenous input), and (2) from an accretionary wedge (undifferentiated magmatic arc-like input).

The subduction processes were initiated already in the early Middle Jurassic when the accretionary wedge began to form. The closing of the sedimentatary basin and the incorporation of the radiolarian cherts and other fragments characteristic of the mélange into the accretionary prism took place during the Late Jurassic when the peripheral foreland basin (piggyback basin) was also created. That basin was filled up with the Lower Cretaceous turbidites. The collisional closing of this part of the Tethys occured in the early Late Cretaceous.

Acknowledgments: This work was supported by the Ministry of Science, Education and Sport of the Republic of Croatia (Basic Geochemical Mapping — Project No. 0181006). We would like to thank Dr. Jozef Michalík (Bratislava, Slovak Republic), Dr. Zbigniew Sawlowicz (Krakow, Poland) and Dr. Paulian Dumitrica (Gümlingen, Switzerland) for very helpful and critical comments which have improved the quality of the paper.

References

Adachi M., Yamamoto K. & Sugisaki R. 1986: Hydrothermal chert and associated siliceous rocks from the northern Pacific: Their geological significance as indication of ocean ridge activity. *Sed. Geol.* 47, 125–148.

Aitchison J. 1986: The statistical analysis of compositional data. *Chapman and Hall*, 1–416.

Allen P.A. & Allen J.R. 1990: Basin analysis. *Blackwell Scientific Publications*, 1–451.

Andreozzi M., Dinelli E. & Tateo F. 1997: Geochemical and mineralogical criteria for the identification of ash layers in the stratigraphic framework of a foredeep; the early Miocene Mt. Cervarola sandstones, northern Italy. *Chem. Geol.* 137, 23–39.

Babić L.J., Hochuli P.A. & Zupanič J. 2002: The Jurassic ophiolitic mélange in the NE Dinarides: dating, internal structure and geotectonic implications. *Eclogae Geol. Helv.* 95, 263–275.

Babić L.J. & Zupanič J. 1973: Uppermost Jurassic and Early Cretaceous deposits on Mt. Ivanščica (Northern Croatia). *Geol. Vjes.* 26, 267–272 (in Croatian).

Baltuck M. 1982: Provenance and distribution of Tethyan pelagic and hemipelagic siliceous sediments, Pindos Mountains, Greece. *Sed. Geol.* 31, 63–88.

Barrett T.J. 1981: Chemistry and mineralogy of Jurassic bedded chert overlying ophiolites in the North Apennines, Italy. *Chem. Geol.* 34, 289–317.

Basch O. 1981: Basic geological map 1:100,000 Sheet Ivanić Grad. *Inst. za Geol. Istraž.* Zagreb, *Sav. geol. Zavod,* Beograd.

Basch O. 1983: Explanatory notes for Sheet Ivanić Grad. *Inst. za Geol. Istraž.* Zagreb, *Sav. Geol. Zavod,* Beograd 1–66 (in Croatian with English summary).

Basch O. 1995: Geological map of Medvednica Mt. (1:75,000). In: Šikić K. (Ed.): Geological Guide of the Medvednica Mt. *Inst. za Geol. Istraž. and INA-Naftaplin*, Zagreb.

Baumgartner P.O., Bartolini A., Carter E.S., Conti M., Cortese G., Danelian T., De Wever P., Dumitrică-Jud R., Goričan Š., Guex J., Hull D.M., Kito N., Marcucci M., Matsuoka A., Murchey B., O'Dogherty L., Savary J., Vishnevskaya V., Widz D. & Yao A. 1995: Middle Jurassic to Early Cretaceous radiolarian biochronology of Tethys based on Unitary Association. In: Baumgartner P.O., O'Dogherty L., Goričan Š., Urquhart E., Pillevuit A. & De Wever P. (Eds.): Middle Jurassic to Lower Cretaceous radiolaria of Tethys: occurrences, systematics, biochronology. *Mém. Géol.* 23, 1013–1038.

Berner R.A. 1973: Phosphate removal from seawater by adsorption on volcanic ferric oxides. *Earth Planet. Sci. Lett.* 18, 77–86.

Bostrom K. 1976: Particulate and dissolved matter as sources for pelagic sediments. *Stockholm Contr. Geol.* 30, 16–79.

Crnjaković M. 1987: Sedimentology of Cretaceous and Paleogene clastics of Mts. Medvednica, Ivanščica and Žumberak. *Unpubl. Phil. Thesis, University of Zagreb, Faculty of Natural and Mathematic Sciences*, 1–91 (in Croatian with English summary).

Crnjaković M. 1989: Lower Cretaceous shalow water sediments of Medvednica Mt. *Acta Geol.* 19, 2, 61–93 (in Croatian with English summary).

Dasgupta H.C., Sambasiva Rao V.V. & Krishna C. 1999: Chemical environments of deposition of ancient iron- and manganese-rich sediments and cherts. *Sed. Geol.* 125, 83–98.

Di Leo P., Dinelli E., Mongelli G. & Schiattarella M. 2002: Geology and geochemistry of Jurassic pelagic sediments, Scisti silicei Formation, southern Apennines, Italy. *Sed. Geol.* 150, 229–246.

Girty G.H., Ridge D.L., Knaack C., Johnson D. & Al-Riyami R.K. 1996: Provenance and depositional setting of Paleozoic chert and Argillite, Sierra Nevada, California. *J. Sed. Res.* 66, 1, 107–118.

Gorjanović-Kramberger D. 1908: Geological map and explanatory notes sheet Zagreb (Zone 22, COL. XIV). *Naklada kr. zemaljske vlade,* 1–75 (in Croatian).

Gromet L.P., Dymek R.F., Haskin L.A. & Korotev R.L. 1984: The "North American shale composite": its compilation, major and trace element characteristics. *Geochim. Cosmochim. Acta* 48, 2469–2482.

Gundlach H. & Marchig V. 1982: Ocean Floor "Metalliferous sediments" — two possibilities for genesis. In: Amstutz G.C., El Goresy A., Frenzel G., Kluth C., Moh G., Wauschkuhn A. & Zimmermann R.A. (Eds.): Ore genesis — the state of the art. *Springer Verlag,* Berlin–Heidelberg, 200–210.

Haas J., Császár G., Kovács S. & Vörös A. 1990: Evolution of the Western Part of the Tethys as reflected by the geological formations of Hungary. *Acta Geod. Geoph. Mont. Hung.* 25, 3–4, 325–344.

Haas J., Kovács S., Krystyn L. & Lein R. 1995: Significance of Late Permian-Triassic facies zones in terrane reconstructions in the Alpine-North Pannonian domain. *Tectonophysics* 242, 19–40.

Haas J., Mioč P., Pamić J., Tomljenović B., Árkai P., Bérczi-Makk A., Oroknai B., Kovács S. & Felgenhauer E.-R. 2000: Complex structural pattern of the Alpine-Dinaridic-Panonnian triple junction. *Int.*

J. Earth Sci. 89, 2, 377–389.

Halamić J. 1998: The lithostratigraphic characterisation of Jurassic and Cretaceous sediments with ophiolite of Mts. Medvednica, Kalnik, and Ivančćica. *Unpubl. Phil. Thesis, University of Zagreb, Faculty of Natural and Mathematics Sciences*, 1–180 (in Croatian with English summary).

Halamić J. & Goričan Š. 1995: Triassic radiolarites from Mts. Kalnik and Medvednica (Notrhwestern Croatia). *Geol. Croatica* 48, 2, 129–146.

Halamić J., Goričan Š. & Slovenec D. 1995: Pelagic siliceous sediments of North-Western part of Medvednica Mt. *1. Croatian Geological Congress*, Proceedings, 36–36 (in Croatian).

Halamić J., Goričan Š., Slovenec Da. & Kolar-Jurkovšek T. 1999: Middle Jurassic Radiolarite-Clastic Succession from the Medvednica Mt. (NW Croatia). *Geol. Croatica* 52, 1, 29–57.

Halamić J., Marchig V. & Goričan Š. 2001: Geochemistry of Triassic radiolarian cherts in North-Western Croatia. *Geol. Carpathica* 52, 6, 327–342.

Haskin M.A. & Haskin L.A. 1966: Rare Earths in European shales: a redetermination. *Science* 154, 507–509.

Herak M. 1986: A new concept of geotectonics of the Dinarides. *Acta Geol*. 16, 1, 1–42.

Herak M., Jamičić D., Šimunić A. & Bukovac J. 1990: The northern boundary of the Dinarides. *Acta Geol*. 20, 1, 5–27.

Jenkyns H.C. & Winterer E.L. 1982: Paleoceanography of Mesozoic ribbon radiolarites. *Earth Planet. Sci. Lett.* 60, 351–375.

Kato Y., Nakao K. & Isozaki Y. 2002: Geochemistry of Late Permian to Early Triassic pelagic cherts from southwest Japan: implications for an oceanic redox change. *Chem. Geol*. 182, 15–34.

Kovács S., Császár G., Galácz A., Haas J., Nagy E. & Vörös A. 1988: The Tisza Superunit was originally part of the North Tethyan (European) margin. In: Rakús M., Dercourt J. & Nairn A.E.M. (Eds.): Evolution of the Northern margin of Tethys: the results of IGCP Project 198. *Mém. Soc. Géol. France* 2, 81–100.

Kunimaru T., Shimizu H., Takahashi K. & Yabuki S. 1998: Differences in geochemical features between Permian and Triassic cherts from the Southern Chichibu terrane, southwest Japan: REE abudances, major element compositions and Sr isotopic ratios. *Sed. Geol*. 119, 195–217.

Manetti P., Peccerillo A. & Poli G. 1979: Rare earth element distribution in jurassic siliceous rocks from northern Apennines (Italy). *Mineral. Petrogr. Acta* 23, 87–98.

Marchig V., Gundlach H., Möller P. & Schley F. 1982: Some geochemical indicators for discrimination between diagenetic and hydrothermal metalliferous sediments. *Mar. Geol*. 50, 241–256.

McLennan S.M. 1989: Rare Earth elements in sedimentary rocks: influence of provenance and sedimentary processes. In: Ipin B.R. & McKay G.A. (Eds.): Geochemistry and mineralogy of the rare Earth elements. *Rev. in Mineralogy* 21, 169–200.

McLennan S.M., Hemming S., McDaniel D.K. & Hanson G.N. 1993: Geochemical approaches to sedimentation, provenance, and tectonics. In: Johnsson M.J. & Basu A. (Eds.): Precesses controlling the composition of clastic sediments. *Geol. Soc. Amer*., *Spec. Pap.* 284, 21–40.

Murray R.W. 1994: Chemical criteria to identify the depositional environment of chert: general principles and applications. *Sed. Geol.* 90, 213–232.

Murray R.W., Buchholtz ten Brink M.R., Jones D.L., Gerlach D.C. & Russ III G.P. 1990: Rare Earth elements as indicators of different marine depositional environments in chert and shale. *Geology* 18, 268–271.

Murray R.W., Buchholtz ten Brink M.R., Brumsack H.J., Gerlach D.C. & Russ III G.P. 1991: Rare Rarth elements in Japan Sea sediments and diagenetic behavior of Ce/Ce*: results from ODP Leg 127. *Geochim. Cosmochim. Acta* 55, 2453–2466.

Murray R.W., Jones D.L. & Buchholtz ten Brink M.R. 1992a: Diagenetic formation of bedded chert: Evidence from chemistry of chert-shale couplet. *Geology* 20, 271–274.

Murray R.W., Buchholtz ten Brink M.R., Gerlach D.C., Russ III G.P. & Jones D.L. 1992b: Rare Earth, major, and trace element comopsition of Monterey and DSDP chert and associated host sediment: assessing the influence of chemical fractionation during diagenesis. *Geochim. Cosmochim. Acta* 56, 2657–2671.

Murray R.W., Buchholtz ten Brink M.R., Gerlach D.C., Russ III, G.P. & Jones D.L. 1992c: Interoceanic variation in the rare earth, major, and trace element depositional chemistry of chert: Perspectives gained from the DSDP and ODP record. *Geochim. Cosmochim. Acta* 56, 1897–1913.

Ori G.G. & Friend P.F. 1984: Sedimentary basins, formed and carried piggyback on active thrust sheets. *Geology* 12, 475–478.

Pamić J. & Tomljenović B. 1998: Basic geological data on the Croatian part of the Zagorje-Mid-Transdanubian Zone. *Acta Geol. Hung.* 41, 389–400.

Pamić J., Tomljenović B. & Balen D. 2002: Geodynamic and petrogenetic evolution of Alpine ophiolites from the central and NW Dinarides: an overview. *Lithos* 65, 113–142.

Pilar Đ. 1881: Grundzüge der Abyssodynamik. *Commisions-Verl. d. Universitäts-Buchhandlung (Albrecht & Fiedler)*, Zagreb, 1–220 (in German).

Rangin C., Steinberg M. & Bonnot-Courtois C. 1981: Geochemistry of the Mesozoic bedded chert of Central Baja California (Vizcaino-Cedros-San Benito): implications for paleogeographic reconstruction of an old oceanic basin. *Earth Planet. Sci. Lett*. 54, 313–322.

Ruitz-Ortiz P.A., Bustillo M.A. & Molina J.M. 1989: Radiolarite sequences of the Subbetic, Betic Cordillera, Southern Spain. In: Hein J.R. & Obradović J. (Eds.): Siliceous deposits of the Tethys and Pacific regions. *Springer Verlag*, 107–127.

Shimizu H. & Masuda A. 1977: Cerium in chert as an indication of marine environment of its formation. *Nature* 266, 346–348.

Shimizu H., Kunimaru T., Yoneda S. & Adachi M. 2001: Sources and depositional environments of some Permian and Triassic cherts: significance of Rb-Sr and Sm-Nd isotopic and REE abundance data. *J. Geol.* 109, 105–125.

Stampfli G.M. & Borel G.D. 2004: The TRANSMED transect in space and time: constraints on the paleotectonic evolution of the Mediterranean domain. In: Cavazza W., Roure F., Spakman W., Stampfli G.M. & Ziegler P.A. (Eds.): The TRANSMED Atlas: the Mediterranean region from crust to mantle. *Springer Verlag*, (in print).

Sugisaki R. 1984: Relation between chemical composition and sedimentation rate of Pacific Ocean-floor sediments deposited since the middle Cretaceous: Basic evidence for chemical constraints on depositional environments of ancient sediments. *J. Geol*. 92, 235–259.

Sugisaki R., Yamamoto K. & Adachi M. 1982: Triassic bedded cherts in central Japan are not pelagic. *Nature* 298, 644–647.

Sugitani K., Yamamoto K., Wada H., Binu-Lal S.S. & Yoneshige M. 2002: Geochemistry of Archean carbonaceous cherts deposited at immature island-arc setting in the Pilbara Block, Western Australia. *Sed. Geol.* 151, 45–66.

Swan A.R.H. & Sandilands M. 1996: Introduction to geological data analysis. *Blackwell Science,* Oxford, 1–446.

Šikić K. 1995: Review of the geology of the Medvednica Mt. In: Šikić K. (Ed.): Geological guide of Medvednica Mt. *Inst. Geol., INA-Naftaplin* 7–30 (in Croatian).

Šikić K., Basch O. & Šimunić A. 1977: Basic geological map 1:100,000 Sheet Zagreb. *Inst. za Geol. Istraž.,* Zagreb*, Sav. Geol. Zavod*, Beograd.

Šikić K., Basch O. & Šimunić A.N. 1979: Basic geological map 1:100,000, explanatory notes sheet Zagreb. *Inst. za Geol. Istr*., Zagreb, *Sav. Geol. Zavod,* Beograd, 1–81 (in Croatian with English summary).

Taylor S.R. & McLennan S.M. 1985: The continental crust: its composition and evolution. *Blackwell,* Oxford–London–Edinburg–Boston–Palo Alto–Melbourne, 1–312.

Wilson M. 1989: Igneous petrogenesis — a global tectonic aproach. *Unwin Hyman,* London, 1–465.